IRAQI Academic Scientific Journals
Samarra Journal of Pure and Applied Science
SJPAS
www.sjpas.com
p ISSN: 2663-7405
e ISSN: 2789-6838

Green Synthesis of Silver Nanoparticles Using Lemon Peels for Fabrication of an Electrochemical Sensor for Sulfamethoxazole Detection

Marwan Hamid Lateef [1*], Shatha Younus Yahya Alsamarri [2]
1- Department of Applied Chemistry, College of Applied Science, University of Samarra, Iraq
2- Department of Chemistry, Collage of Science, Tikrit University, Iraq

https://doi.org/10.54153/sjpas.2026.v8i1.1212

Article Information
Received: 27/04/2025
Revised: 24/05/2025
Accepted: 06/06/2025
Published: 10/04/2026

Keywords:
Sulfamethoxazole, Silver Nanoparticles, Green Synthesis, Coated Sensor, and Drug Detection

Corresponding Author

E-mail: marwan.hamid@st.tu.edu.iq
Mobile: 07711717420

Abstract

A green electrochemical sensor was developed for the selective detection of sulfamethoxazole (SMX), a sulfonamide antibiotic, using silver nanoparticles (AgNPs) synthesized via an eco-friendly route employing lemon peel extract. The AgNPs were complexed with SMX to form ion-pair structures (SMX-AgNPs), which were subsequently incorporated into a graphite-based ion-selective electrode (ISE). Structural and morphological characterization of the synthesized nanomaterials was performed using UV–Vis spectroscopy, scanning electron microscopy (SEM), energy-dispersive X-ray spectroscopy (EDX), and X-ray diffraction (XRD), confirming the formation of crystalline, nanoscale particles. The fabricated electrode demonstrated a wide linear response range (1×10^{-1} to 1×10^{-7} M), fast response time, and high reproducibility, with operational stability maintained over a 65-day period. The sensor exhibited excellent sensitivity and selectivity, enabling accurate quantification of SMX in pharmaceutical formulations. These results underscore the potential of green-synthesized AgNPs in advancing low-cost, sustainable sensing technologies for drug monitoring.

1-Introduction

Sulfamethoxazole (SMX) (fig.1), the first sulfonamide antibiotic commonly used, is a broad-spectrum antibiotic [1]. Sulfamethoxazole (SMX) is a member of the Sulfanilamide class. Its chemical name is 4-amino-N-(5-methyl-1,2-oxazole-3-yl)benzene sulfonamide [2]. SMX Eliminates inflammation and treats infections in humans and animals [3]. SMX inhibits bacterial growth by interfering with folic acid synthesis. It acts as a structural analog of para-aminobenzoic acid (PABA), a key intermediate used by bacteria, viruses, and plants to produce folic acid. By mimicking PABA, SMX competes for the active site of the enzyme involved in folic acid production, thereby blocking the incorporation of PABA. This inhibition disrupts the synthesis of folic acid, which is essential for DNA production, ultimately preventing bacterial replication [4]. Due to its extensive clinical use and pharmacological importance, there is an increasing need for reliable, efficient, and cost-effective methods to

quantify SMX in pharmaceutical formulations and environmental samples. Nanotechnology is one of the most rapidly developing fields in science with a broad impact on different aspects of human life[5]. Electroanalytical methods provide a powerful sensing platform, due to the several advantages of instrumental simplicity, affordability cost, and flexibility, and exceed many traditional analysis. [6]. Electrochemical sensors are an important branch of chemical sensors and work by measuring the electrical output signal derived from a chemical reaction [7]. These benefits have been improved by introducing different nanomaterials, NPs as metals, oxides, carbon, polymers, nanoclays, and composites[8]. Ion-selective electrodes (ISEs) are powerful analytical tools for the study of the target analyte in various fields. The application of ISEs is a special analytical tool that has advantages over other traditional methods in low cost, easy operation, and miniaturization[9].

The synthesis of nanomaterials has significantly progressed during the past decade, and sensors integrated with nanomaterials have exhibited excellent performance because of their size-dependent properties, the high surface area to volume ratio, changeable physical behavior, and the specific surface chemistry suitable for interaction with target analytes. Their high surface area allows for greater analyte adsorption, thereby enhancing sensitivity. Additionally, their excellent electrical conductivity facilitates faster electron transfer, improving the signal response. NMs can also be easily functionalized to increase selectivity toward specific target molecules[10].

Silver nanoparticles (AgNPs) have been extensively used for sensing, antibacterial, anticoagulant, anticancer, orthopedic, and thrombolytic applications, medication transport, medical devices, and diagnostics. Their significance arises from their catalytic activity, optical and thermal characteristics, chemical stability, thermal stability, and antibacterial efficacy [11]. The bio-friendly preparation of AgNPs is superior to physical and chemical approaches. Combining the plant-derived secondary metabolites' inherent properties and the one-step experimental setup stabilizes and reduces bulk silver to AgNPs. The true meaning of biosynthesized methods is the application of eco-friendly synthetic agents or natural deposits that are less toxic, compatible with humans and the environment, and can be used more extensively[12]. Unlike physical and chemical methods, biogenic AgNPs are, by definition, bio-friendly since they are prepared using live organisms or their byproducts. Due to the inherent properties of plant-derived secondary metabolites and the simplicity of a one-step experimental setup, bulk silver ions are simultaneously reduced and stabilized to form AgNPs. Such biosynthetic approaches have many additional advantages, such as cost, energy efficiency, and scalability. They offer a safer alternative by removing the need for hazardous reducing or capping agents, lowering environmental toxicity, and improving biocompatibility. Additionally, the use of natural extracts also allows a more sustainable and renewable approach because it leads to nanoparticles with improved stability and functional surface groups that can enhance the biocompatibility and performance of the synthesized products used in biomedical and sensing applications. In other words, such green synthesis is safe for human health and better integrates with the principles of green chemistry [11].

This research was aimed at developing an eco-friendly, cost-effective, and highly effective electrochemical sensor for the detection of SMX based on silver nanoparticles prepared through the green approach using the extract of lemon peel. The silver nanoparticles

(AgNPs) were utilized to form composites and to coat the graphite-based ion-selective electrode. These Enhancement improves the sensor's sensitivity, selectivity, and response time. The suggested analytical method is more straightforward than current techniques, offering minimal environmental impact, lower reagent usage, and quicker, highly precise on-site analysis. As a result, the approach is quite suitable for the standard quality control of pharmaceuticals and environmental monitoring of SMX.

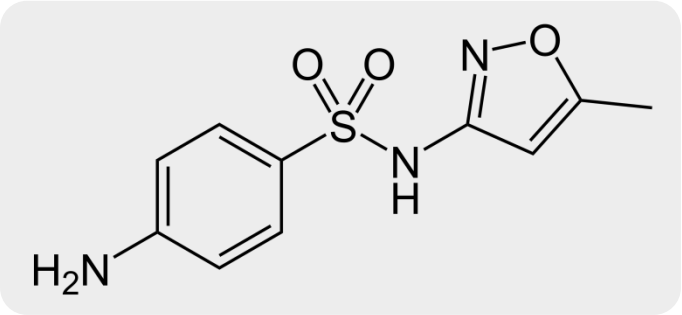

Fig. 1: *The structure of sulfamethoxazole*

2. Materials and Methods

2.1. Instrumentations

1. PH meter, Jenway 3310, England
2. Calomel Electrode, Me-SC900, England
3. Polyethylene (PE) Tubing
4. Whatman filter paper No.1
5. UV spectrophotometer, SHIMADZU, Japan
6. Magnetic stirrer and Hot plate, FTHPM-10, Korea
7. Oven, KAROL, Korea

2.2. Chemicals and Reagents

2.2.1. Standard Stock Solution of Sulfamethoxazole (SMX)

Stock solutions were prepared using distilled water as the primary solvent. The reagents included:

- Sulfamethoxazole (SMX, 99% purity): Sourced from SDI, Samara-Iraq.
- Polyvinyl chloride (PVC, 98% purity) and di-n-butyl phthalate (DBP, 98% purity): Obtained from Fluka.
- Tetrahydrofuran (THF, 99% purity)) and silver nitrate (99% purity): Obtained from Sigma.

To prepare a 0.1 M SMX stock solution, 2.5328 g of SMX was dissolved in acetone and diluted with water to a total volume of 100 mL in a volumetric flask. Standard solutions were prepared by systematically diluting the 0.1 M stock solution to obtain concentrations ranging from 1.0×10^{-2} M down to 1.0×10^{-7} M.

2.3. Sample Preparation

Ten tablets of Metheprim (Sulfamethoxazole 400 mg, Trimethoprim 80mg) (SDI, Samara-Iraq) weighing 5.388 g were finely ground and thoroughly mixed. A solution of Metheprim (400 mg) was prepared by accurately weighing 3.411 g of the compound and dissolving it in acetone. The resulting solution was quantitatively transferred to a 100 mL volumetric flask and diluted to the mark with distilled water.

The solution was filtered through Whatman filter paper to remove any insoluble substances. The resulting filtrate was transferred to a 100 mL volumetric flask, and distilled water was added to reach the final volume. The concentration of the stock solution was 10^{-1} M, and appropriate serial dilutions with distilled water prepared other concentrations.

Similar procedures were followed for Supreme D. S (Sulfamethoxazole 800 mg) (Janta, India). The active pharmaceutical ingredient was dissolved in acetone and diluted accordingly to achieve the desired concentrations.

2.4. Preparation of lemon peel extract

The fresh lemon peels (fig.2) were thoroughly washed with distilled water to remove dust and organic impurities and then dried on paper towels. We diced the peels into small parts. Approximately 10 grams of peels were heated with 200 ml of deionized water at 30 to 40 °C for 20 minutes. A pale yellow extract was obtained. The extract was subsequently cooled and filtered using Whatman No. 1 filter paper. The extract was collected and preserved at 4 °C for further research [13].

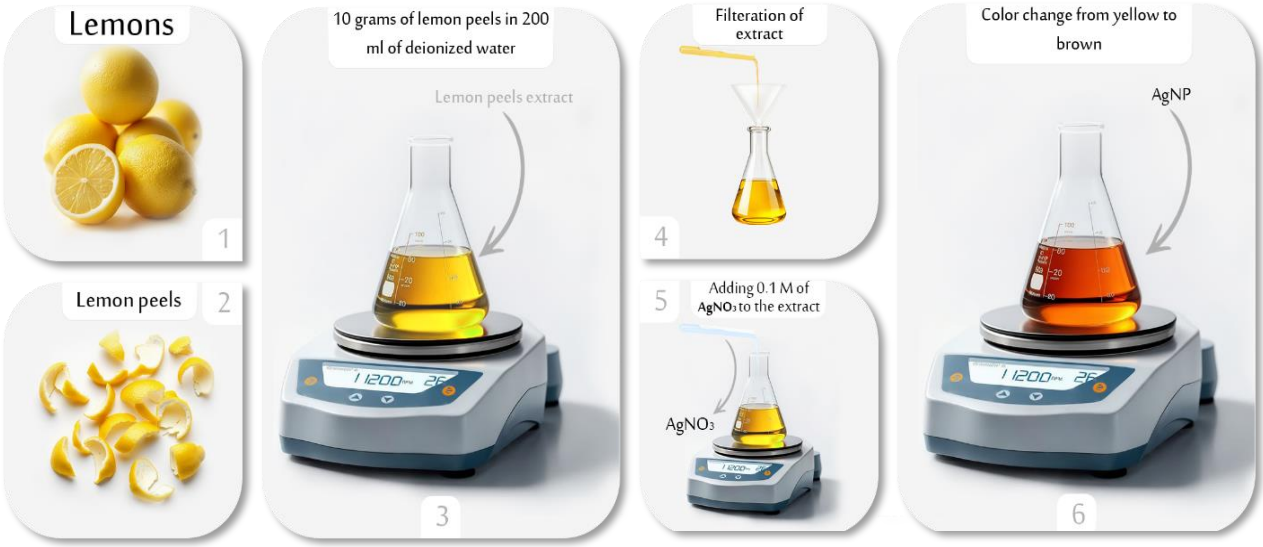

Fig. 2*: Schematic Representation of the Green Synthesis of Silver Nanoparticles (AgNPs)*

2.5. Green Synthesis of Silver Nanoparticle Using Plant Extract

50 ml of prepared plant extract was combined with 50 ml of 0.1 M silver nitrate solution at approximately 50-60 °C until a colour change in the mixture was observed.

A colour shift is usually observed when silver ions are reduced to silver nanoparticles, as evidenced by AgNPs forming, which change from pale yellow to brown [14].

2.6. Ion-Pairs Preparation

As shown in Fig.3, a brown precipitate indicating SMX-AgNPs complexation was formed when 50 mL of a 0.1 M sulfamethoxazole (SMX) drug solution was mixed with 100 mL of silver nanoparticle (AgNPs) solution. Whatman No.1 filter paper was used to separate the precipitate, which was then air-dried at room temperature for 48 hours.

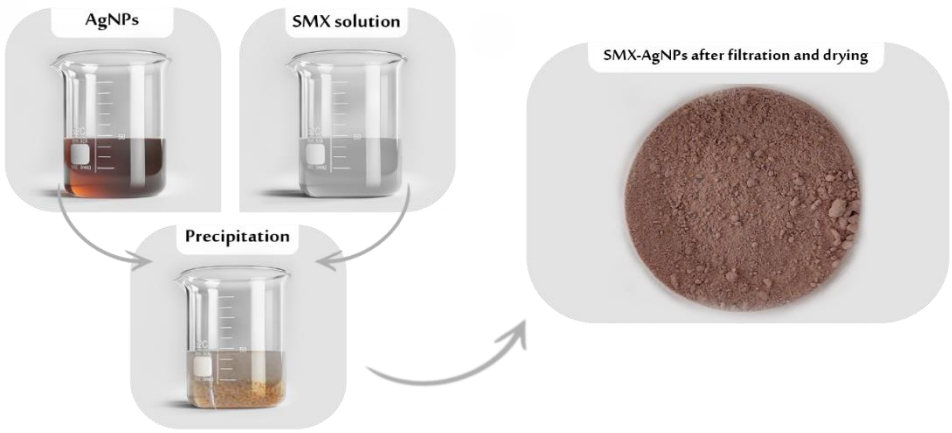

Fig. 3: *Formation of a brown precipitate of SMX-AgNPs*

2.7. Fabrication of the Coated Carbon Sensor

The coated carbon sensor was prepared using a high-purity carbon rod fully covered with polyethylene tube, leaving only about 0.5 cm of the rod exposed as the sensing surface. The active membrane was formed by repeatedly dip-coating the exposed end of the electrode into a membrane-forming solution. This solution was prepared by mixing 0.1 g of the synthesized ion-pair complex (SMX-AgNPs), 0.19 g of polyvinyl chloride (PVC), 0.25 mL of dibutyl phthalate (DBP) as a plasticizer, and 5 mL of tetrahydrofuran (THF) as the solvent. After each dip, the electrode was air-dried for five minutes to ensure uniform membrane formation. The opposite end of the carbon rod remained uncovered to allow for electrical connection. The structural components of the resulting coated carbon sensor are illustrated in Fig. 4.

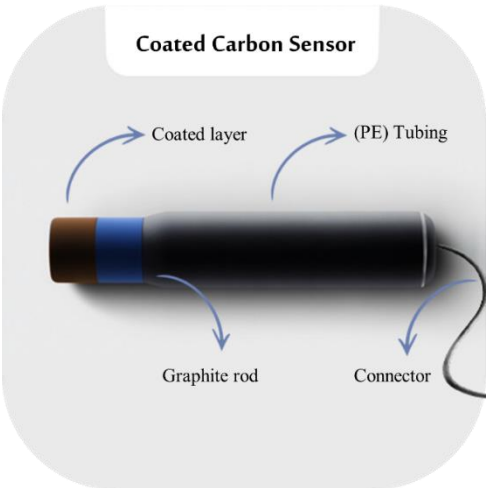

Fig. 4: *The basic parts of the coated carbon sensor electrode*

3. Results and discussion

3.1. Characterization

3.1.1. UV-Visible Spectroscopy for silver nanoparticles

UV-vis spectroscopy is a reliable and effective technique for the first characterization of synthesized nanoparticles. It is used to measure the production and stability of AgNPs [13]. Due to their distinctive optical characteristics, silver nanoparticles (AgNPs) exhibit strong interactions with specific wavelengths of light, particularly through surface plasmon resonance phenomena [14]. The optical properties of the synthesized AgNPs were evaluated using UV–Vis spectrophotometry over a wavelength range of 200 to 800 nm. As illustrated in Fig. 5, a characteristic absorption peak was observed at 463 nm. This peak falls within the typical surface plasmon resonance range of 440-480 nm, confirming the successful formation and stability of the silver nanoparticles [15].

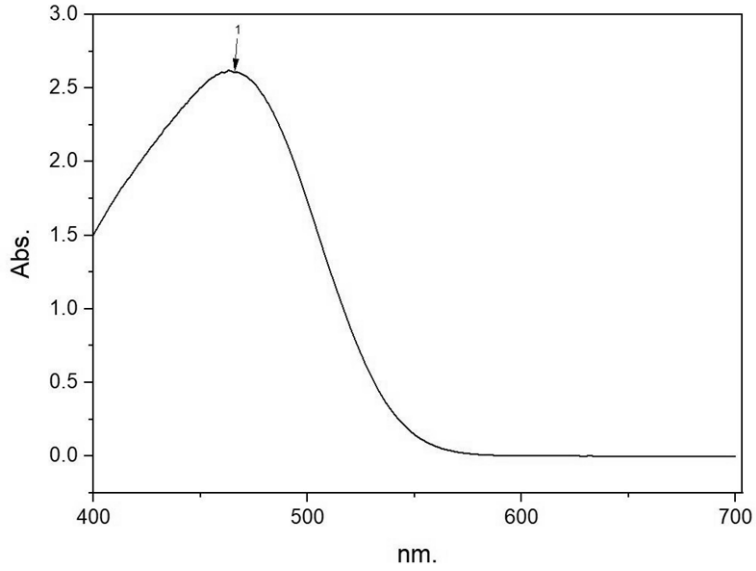

Fig. 5: *UV–Vis Spectral Analysis of Silver Nanoparticles*

3.1.2. Scanning Electron Microscopy (SEM)

Scanning electron microscopy (SEM) is a powerful imaging technology that facilitates high-resolution imaging and the study of materials' surface morphology, structure, and composition. The morphology and composition of nanomaterials significantly influence their overall properties. In contrast, SEM offers substantial advantages in examining the microscopic morphology of materials, making it essential for materials investigation and processing [16].

Fig. 6 displays the scanning electron microscopy (SEM) of silver nanoparticles synthesized from lemon peel extract and (SMX-AgNPs). SEM analysis at scales of 200 nanometers and 10 micrometers reveals particles distributed across the examined surface, predominantly exhibiting spherical or semi-spherical shapes.

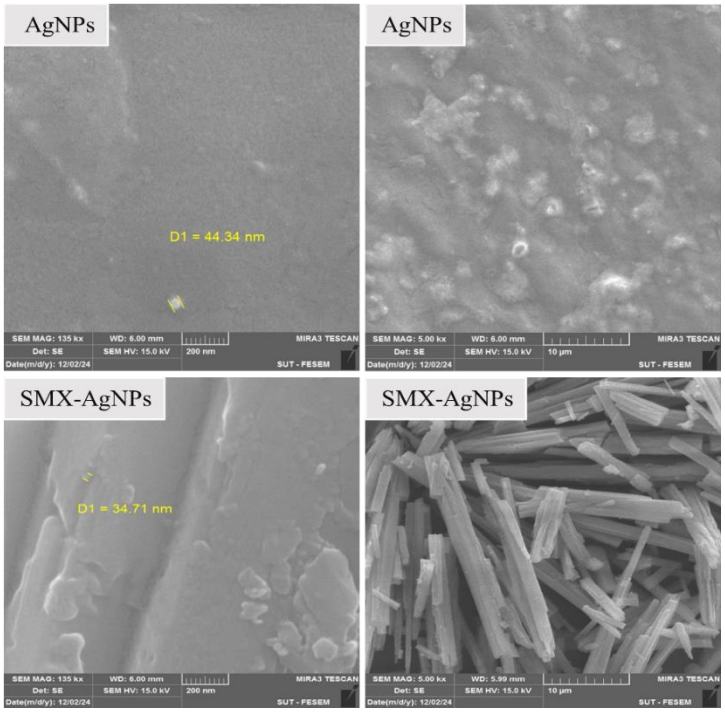

Fig. 6: *SEM of silver nanoparticles synthesised from lemon peel extract and (SMX-AgNPs)*

3.1.3. X-ray Diffraction (XRD).

Techniques like XRD, which provide information on crystal structure and lattice parameters, are extensively utilized for characterizing the crystalline characteristics of Ag nanoparticles, as shown (Fig.7; Table 1) [17]. This technique relies on broadening X-ray diffraction peaks and yields insights into microstructural characteristics, including crystallite size, defects, and lattice strains, which are critical to material behavior, as shown(Fig.8; Table 2) [18]. XRD analysis was used to study the structure and size of the silver nanoparticles (AgNPs). XRD pattern showed clear peaks at 2θ values of 32.23°, 48.16°, and 67.47°, which match the typical planes of face-centred cubic (FCC) silver [19]. The strongest peak at 32.23° indicates the main crystal orientation.

The measured d-spacing values agree with standard data for metallic silver, confirming the crystalline structure of the particles.

Using the Scherrer equation[20], the particle sizes were calculated from the peak widths. The sizes ranged from 14.43 to 16.67 nm, with an average of 15.42 nm, indicating the formation of well-defined nanoscale silver particles.

Table 1: X-ray Diffraction (XRD) Data for AgNPs

Pos. [°2Th.]	Heigh t [cts]	FWHM Left [°2Th.]	d-spacing [Å]	Rel. Int. [%]	D
32.2305	25926	0.2668	2.77515	100.00	14.42
48.160	255	0.37	1.88792	0.98	15.18
67.466	342	0.33	1.38711	1.32	16.66
				Average particle size (nm)	15.42

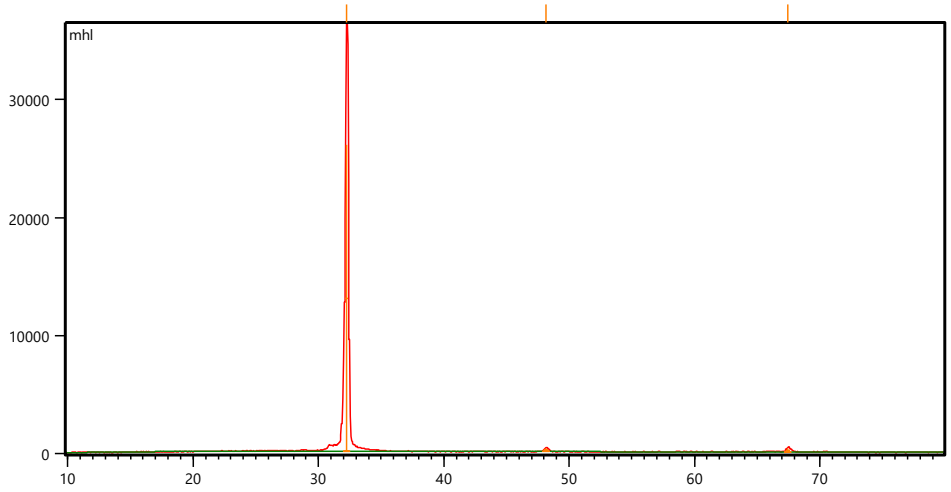

Fig. 7: *X-ray Diffraction (XRD) spectrum for AgNPs*

Table 2: X-ray Diffraction (XRD) Data for SMX-AgNPs

Pos. [°2Th.]	Height [cts]	FWHM Left [°2Th.]	d-spacing [Å]	Rel. Int. [%]	D
11.148	283	0.31	7.93023	100.00	13.92
12.92	62	0.30	6.84649	21.94	13.94
17.25	81	0.34	5.13596	28.51	14.01
21.48	25	2.3	4.13428	8.83	14.10
22.80	52	0.25	3.89648	18.52	14.13
25.94	102	0.86	3.43145	36.07	14.22
26.62	14	0.016	3.34625	4.91	14.24
28.81	59	0.45	3.09594	20.82	14.30
29.48	48	0.52	3.02797	16.87	14.33
32.06	25	1.9	2.78934	8.75	14.42
34.99	27	0.8	2.56206	9.40	14.53
36.88	45	1.1	2.43494	15.77	14.61
43.85	38	0.49	2.06299	13.43	14.94
				Average particle size (nm)	14.11

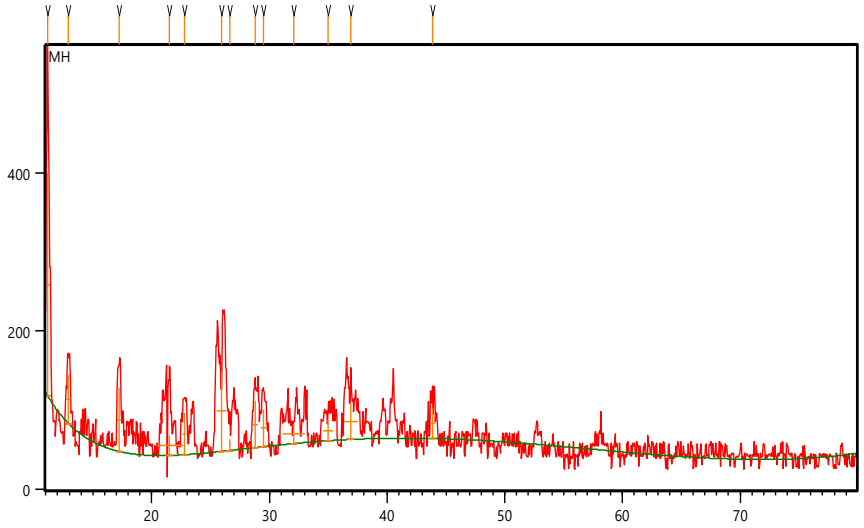

Fig. 8: *X-ray Diffraction (XRD) spectrum for SMX-AgNPs*

3.1.4. Energy dispersive X-ray spectroscopy (EDX)

This technique is a reliable and widely employed chemical characterization and imaging approach[21]. The AgNPs-proven formation is further confirmed by the EDX spectrum in Fig.9, which shows a strong signal in the silver region. The optical absorption peak of metallic silver nanocrystals is generally derived from surface plasmon resonance at approximately 3 keV [22].

In Table 3, silver content, accounting for 61.98 wt%, confirms the successful synthesis of metallic nanoparticles. The prominent silver peaks in the EDS spectrum validate the reduction of Ag^{+} ions to Ag^{0}.

The oxygen and nitrogen content, contributing 22.53 wt% and 15.48 wt%, respectively, can be attributed to the presence of lemon extract in the synthesis process. Lemon extract is rich in organic acids, flavonoids, and other biomolecules that play a dual role as reducing and capping agents [23]. These biomolecules facilitate the reduction of silver ions (Ag^{+}) to metallic silver (Ag^{0}) and subsequently bind to the nanoparticle surface [24].

The EDS spectrum of AgNPs before and after exposure to SMX differs significantly, suggesting a strong interaction. In the spectrum of AgNPs, silver (Ag) is the dominant element, accompanied by minor signals for oxygen (O) and nitrogen (N). After exposure to SMX, new peaks showing carbon (C) and sulfur (S) show up, showing SMX has bound. Moreover, the intensities of nitrogen and oxygen increase while the Ag signal diminishes, indicating surface change. The presence of sulfur, coupled with higher carbon, nitrogen, and oxygen indications, confirms the interaction between SMX and AgNPs.

Table 3: Percent of elements present in the AgNPs

Element	Line Type	Wt %	Atomic %
N	K series	15.48	35.79
O	K series	22.53	45.60
Ag	L series	61.98	18.60
Total		100.00	100.00

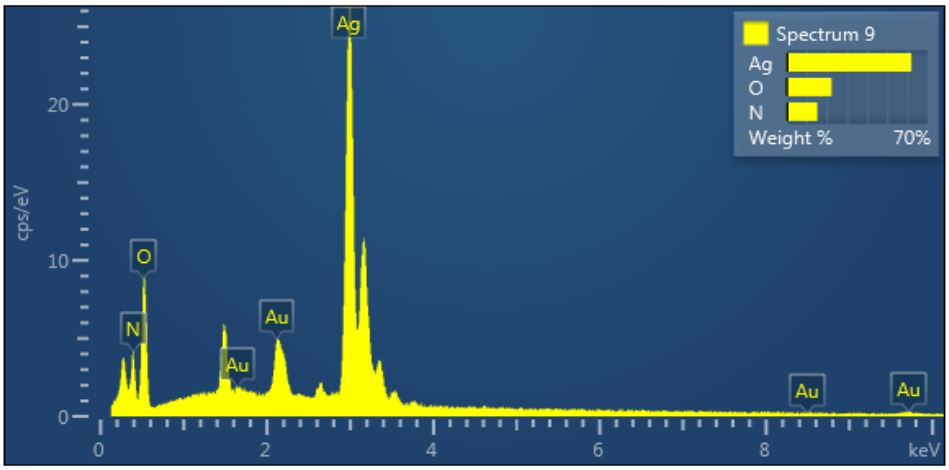

Fig. 9: *EDS-Spectroscopy view showing the synthesis of silver nanoparticles and elemental silver signal in a higher percentage*

Table 4: Percent of elements present in the (SMX- AgNPs)

Element	Line Type	Wt%	Atomic %
C	K series	33.31	52.15
N	K series	16.84	22.61
O	K series	12.62	14.84
S	K series	9.51	5.57
Ag	L series	27.72	4.83
Total		100.00	100.00

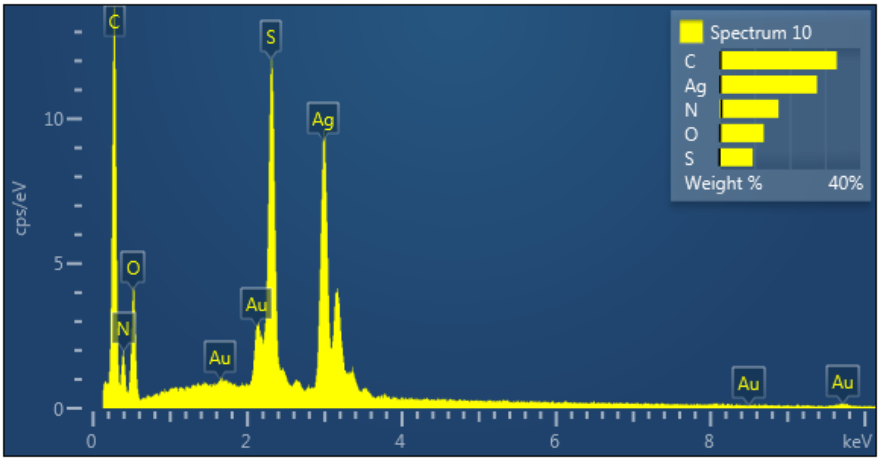

Fig. 10: *EDS-Spectroscopy view showing synthesis (SMX-AgNPs) and elemental silver signal in a higher percentage*

3.2. Study of Optimal Conditions for Nanoelectrodes

3.2.1. Effect of pH

The optimal pH conditions for the efficacy of the synthesized nanoelectrodes were examined by utilizing sulfamethoxazole (SMX) solutions at concentrations of 1×10^{-4} M and 1×10^{-6} M. The pH of the solutions was meticulously adjusted from 3 to 12 through the incremental addition of minimal volumes of HCl or NaOH solutions (0.1–1M). The electrode potential was systematically recorded at each pH value; the results are shown in Fig.11. The nanoelectrode exhibited a stable potential across the entire tested pH range, with only slight fluctuations observed, thereby indicating this range as the optimal condition for the electrode.

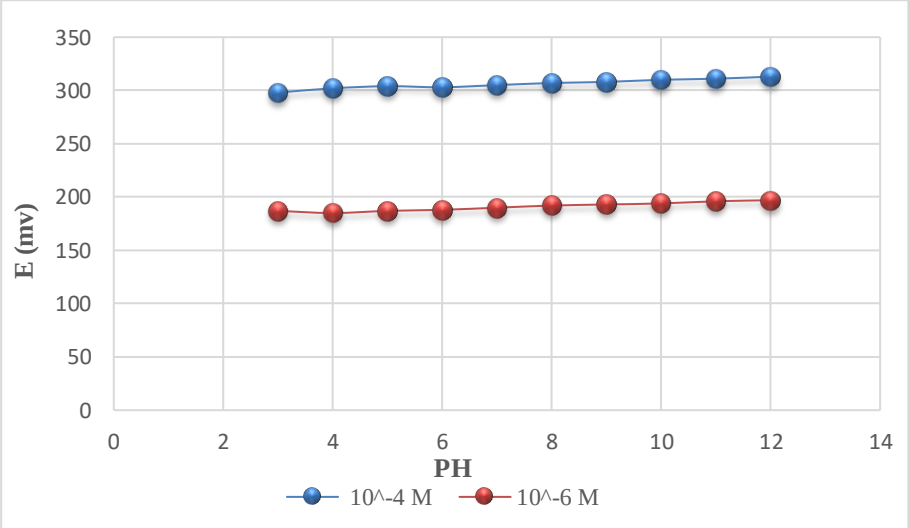

Fig. 11: *Effect of pH*

3.2.2 .Effect of Temperature

The influence of temperature on the electrode potential was evaluated by testing SMX solutions at concentrations of 1×10^{-4} M and 1×10^{-6} M across a temperature range of 20 °C to 50 °C. The electrode response was recorded and plotted to assess thermal behavior (Fig. 12). Although the nanoelectrodes exhibited stable performance across the studied range, the potential measurements at 20 °C showed the most consistent and optimal values. Therefore, 20 ± 1 °C was identified as the optimal operational temperature for the sensor, ensuring minimal error and reliable voltage output under standard laboratory conditions.

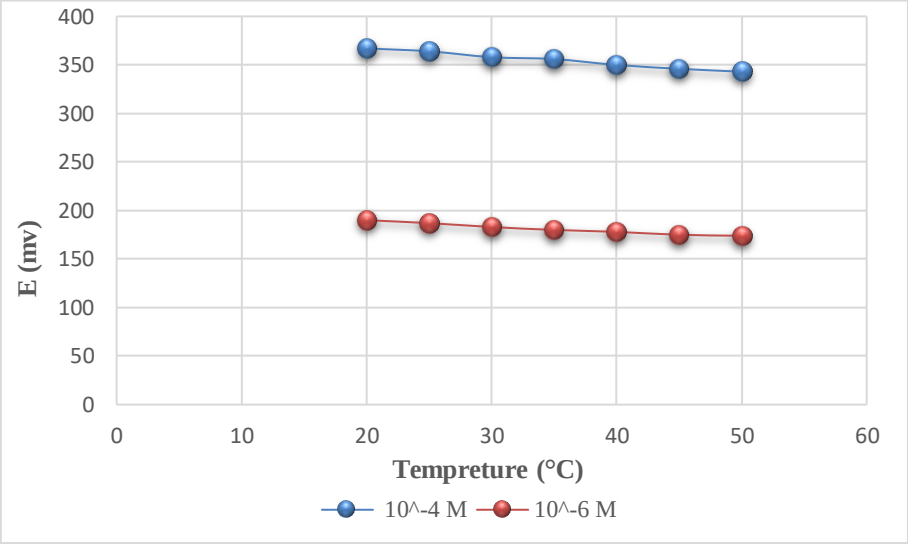

Fig. 12: *Effect of temperature*

3.2.3. Calibration Curve and Detection Limit of the Fabricated Electrode

The electrochemical performance of the synthesized SMX-modified silver nanoparticle electrode (SMX-AgNPs) was evaluated using a calomel reference electrode across a series of SMX standard solutions with concentrations ranging from 1×10^{-1} to 1×10^{-7} M. The potential (E, in mV) was plotted against the negative logarithm of SMX concentration (-log [SMX]), as shown in Fig.13. The resulting calibration curve demonstrated a strong linear response throughout the tested concentration range, with a slope of -59.107 mV per decade. This value closely aligns with the theoretical Nernstian slope, confirming the electrode's high sensitivity and suitability for quantitative detection of SMX.

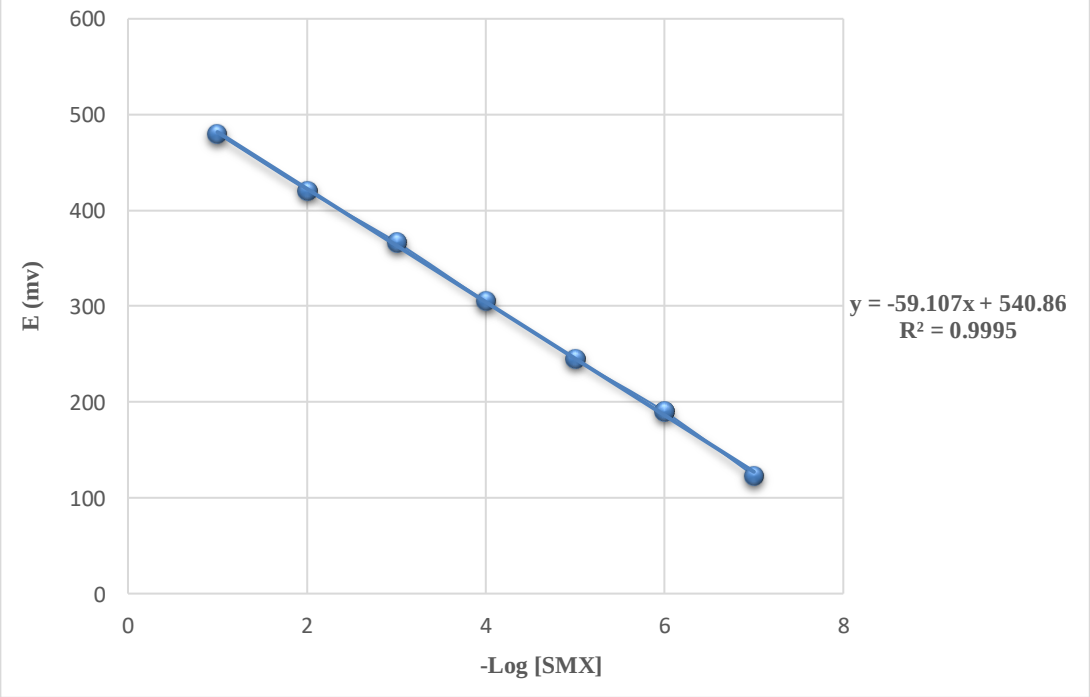

Fig 13: *Calibration curve of (SMX-AgNPs) electrode.*

3.2.4. Lifespan and Response Time

The storage stability of the SMX-AgNP electrode was evaluated through repeated potentiometric measurements conducted several times per week over a period of 65 days. Measurements were carried out under controlled conditions using SMX solutions at the concentration level of 1×10^{-4} M and 1×10^{-6} M over the pH range from 2–12 at a temperature of 25±1°C, and the electrode was kept dry at room ambient temperature between measurements. The stability was determined by observing the end responses over time, with differences less than ±2 mV considered acceptable. The electrode showed constant and reliable performance at both concentrations for 65 days, indicating the long-term stability and durability.

The electrode's response time was studied at different concentrations of SMX. Thus, at a concentration of 1×10^{-7} M, the response time was 29 seconds. Meanwhile, when the concentration of the SMX was 1×10-1 M, the time sharply decreased to 7 seconds. This can be explained by the fact that the higher the concentration of the SMX, the faster it can interact with the electrode, and the signal can be detected (see Fig.14).

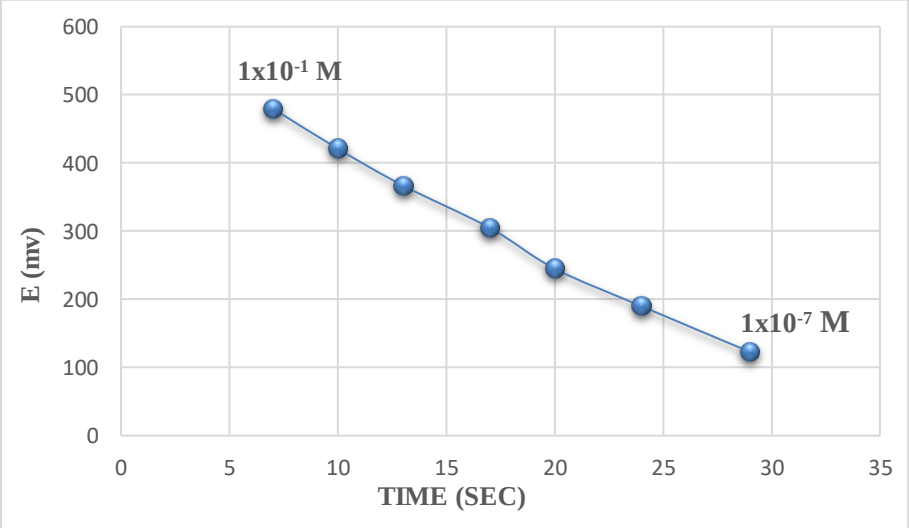

Fig. 14*: Response time of AgNPs-SMX electrode*

3.2.5. Accuracy and Precision

Pure and pharmaceutical formulations of the drug were analyzed at two concentration levels to evaluate the precision and accuracy of the proposed method. Each concentration was tested in five replicates to assess reproducibility. The analytical results presented in Table 5 show low standard deviations and high recovery values, which are also shown in the same table. These results are evidence of excellent precision and accuracy. The results obtained in this investigation sufficiently confirm that the proposed method can be used for quantitative analysis of the drug in pharmaceutical preparations.

3.2.6. Analytical Applications

A direct calibration method was applied to quantify sulfamethoxazole (SMX) in its pure form and pharmaceutical preparations, ensuring the accuracy and reliability of the fabricated electrodes. The analysis results were presented as recovery percentages, reflecting the efficiency of the SMX-AgNP electrode.

The recovery of pure SMX solution was 97.7%, indicating the electrode's applicability for anal-ytical purposes. The SMX-AgNPs electrode was successfully applied to pharmaceutical formulations; the recovery was 98.5% for Metheprim (400 mg) and 99.0% for Supreme (800 mg). These results, presented in Table 5, highlight the electrode's promising ability for accurate and regular monitoring of SMX in different matrices.

Table 5: Evaluation of Recovery and Precision for Sulfamethoxazole (SMX) in Pure and Pharmaceutical Forms

Sample	Taken (mol/L)	Found (mol/L)	Rec%	RSD%
The stock	1×10^{-4}	9.77×10^{-5}	97.7	0.47
Sulfamethoxazole	1×10^{-6}	1.023×10^{-6}	102.3	0.52
Metheprim (400 mg)	1×10-4	9.85×10^{-5}	98.5	0.55
	1×10^{-6}	1.015×10^{-6}	101.5	0.48
Supreme-D.S (800 mg)	1×10^{-4}	0.99×10^{-4}	99	0.51
	1×10^{-6}	1.045×10^{-6}	104.5	0.49
Average of five determinations				

Conclusion

This work has achieved the green synthesis of AgNPs using plant-based extract and further characterized their crystalline nature and nanoscale dimensions by SEM and XRD techniques. The synthesized AgNPs have been effectively combined with SMX to develop stable ion-pair complexes, which were coated with a carbon-based solution. The resulting AgNPs-SMX electrode afforded many analytical characteristics like high sensitivity, stability, reproducibility, and fast response time. It confirms that the sensor developed in this work could be used as a reliable instrument for the detection of SMX in pharmaceutical quality control and environmental samples. The current research highlights the importance of nanomaterials in improving electrochemical sensor abilities in pharmaceutical quality control and clinical applications. Future, it is possible to surface further modification technologies or composite materials examined to optimal selectivity levels and the detection of other drugs and biomedical diagnostics.

References

1. X.-Y. Fan *et al.*, 'Microecology of aerobic denitrification system construction driven by cyclic stress of sulfamethoxazole', *Bioresour. Technol.*, p. 130801, 2024.
2. Ch.Divya *et al.*, 'Sulfamethoxazole Pharmaceutical Dosage Form Quantitative Estimation Using UV-Visible Spectrophotometric Method', May 20, 2024, *Research Square*. doi: 10.21203/rs.3.rs-4433670/v1.
3. S. Li, S. Yan, Z. Tong, X. Yong, X. Zhang, and J. Zhou, 'Assessment of photocatalytic activities of layered double hydroxide@ petrochemical sludge biochar for sulfamethoxazole degradation', *Sep. Purif. Technol.*, vol. 355, p. 129732, 2025.
4. J. Martini, J. O. Ighalo, E. C. Emenike, J. Georgin, and E. Carissimi, 'Degradation of the Antibiotic Sulfamethoxazole by Ozonation: A Comprehensive Review', *CleanMat*, vol. 1, no. 1, pp. 16–51, 2024, doi: 10.1002/clem.14.

5. M. C. Roco and W. S. Bainbridge, 'Societal implications of nanoscience and nanotechnology: Maximizing human benefit', *J. Nanoparticle Res.*, vol. 7, no. 1, pp. 1–13, Feb. 2005, doi: 10.1007/s11051-004-2336-5.
6. B.-R. Adhikari, M. Govindhan, and A. Chen, 'Carbon Nanomaterials Based Electrochemical Sensors/Biosensors for the Sensitive Detection of Pharmaceutical and Biological Compounds', *Sensors*, vol. 15, no. 9, pp. 22490–22508, Sep. 2015, doi: 10.3390/s150922490.
7. M. Madadelahi, F. O. Romero-Soto, R. Kumar, U. B. Tlaxcala, and M. J. Madou, 'Electrochemical sensors: Types, applications, and the novel impacts of vibration and fluid flow for microfluidic integration', *Biosens. Bioelectron.*, vol. 272, p. 117099, Mar. 2025, doi: 10.1016/j.bios.2024.117099.
8. S. Timakwe, S. Ngcobo, R. Smith, and M. Matoetoe, 'Nanoclay composites in electrochemical sensors', *Front. Sens.*, vol. 5, p. 1395853, Oct. 2024, doi: 10.3389/fsens.2024.1395853.
9. M. Cuartero, N. Colozza, B. M. Fernández-Pérez, and G. A. Crespo, 'Why ammonium detection is particularly challenging but insightful with ionophore-based potentiometric sensors – an overview of the progress in the last 20 years', *The Analyst*, vol. 145, no. 9, pp. 3188–3210, 2020, doi: 10.1039/D0AN00327A.
10. M. A. Darwish, W. Abd-Elaziem, A. Elsheikh, and A. A. Zayed, 'Advancements in nanomaterials for nanosensors: a comprehensive review', *Nanoscale Adv.*, vol. 6, no. 16, pp. 4015–4046, 2024, doi: 10.1039/D4NA00214H.
11. D. Bamal *et al.*, 'Silver Nanoparticles Biosynthesis, Characterization, Antimicrobial Activities, Applications, Cytotoxicity and Safety Issues: An Updated Review', *Nanomaterials*, vol. 11, no. 8, p. 2086, Aug. 2021, doi: 10.3390/nano11082086.
12. Vidyasagar, R. R. Patel, S. K. Singh, and M. Singh, 'Green synthesis of silver nanoparticles: methods, biological applications, delivery and toxicity', *Mater. Adv.*, vol. 4, no. 8, pp. 1831–1849, 2023, doi: 10.1039/D2MA01105K.
13. M. Sastry, V. Patil, and S. R. Sainkar, 'Electrostatically controlled diffusion of carboxylic acid derivatized silver colloidal particles in thermally evaporated fatty amine films', *J. Phys. Chem. B*, vol. 102, no. 8, pp. 1404–1410, Feb. 1998, doi: 10.1021/jp9719873.
14. Q. Wu, K. Kremer, S. Gibbons, and A. Kennedy, 'Determination of fluorescence emission and UV-Vis-NIR absorbance for nanomaterials solution using a HORIBA Scientific NanoLog® spectrofluorometer', Engineer Research and Development Center (U.S.), Jun. 2019. doi: 10.21079/11681/32969.
15. G. Annadurai and C. Kannan, 'Green synthesis of Silver Nanoparticle using Elettaria Cardamomom and Assessment of its Antimicrobial Activity', 2012. Accessed: Jan. 31, 2025. [Online]. Available: https://www.semanticscholar.org/paper/Green-synthesis-of-Silver-Nanoparticle-using-and-of-Annadurai-Kannan/47d4478ed3d4368ef8a2f6beabe35da7418a76a6#citing-papers
16. Z. Li and J. Yao, 'Application of scanning electron microscopy in two-dimensional material characterization', *Appl. Comput. Eng.*, vol. 23, pp. 170–176, Nov. 2023, doi: 10.54254/2755-2721/23/20230648.
17. Md. K. H. Shishir *et al.*, 'Transmission Electron Microscopic and X-ray Diffraction Based Study of Crystallographic Bibliography Demonstrated on Silver, Copper and Titanium Nanocrystals: State of the Art Statical Review', *Asian J. Appl. Chem. Res.*, vol. 15, no. 3, pp. 1–19, May 2024, doi: 10.9734/ajacr/2024/v15i3287.

18. P. Mathumba, M. P. Bilibana, O. C. Olatunde, and D. C. Onwudiwe, 'X-ray diffraction profile analysis of green synthesized ZnO and TiO2 nanoparticles', *Mater. Res. Express*, vol. 11, no. 7, p. 075011, Jul. 2024, doi: 10.1088/2053-1591/ad63ff.
19. D. Jain, H. K. Daima, S. Kachhwaha, and S. L. Kothari, 'SYNTHESIS OF PLANT-MEDIATED SILVER NANOPARTICLES USING PAPAYA FRUIT EXTRACT AND EVALUATION OF THEIR ANTI MICROBIAL ACTIVITIES'.
20. F. W. Jones and W. L. Bragg, 'The measurement of particle size by the X-ray method', *Proc. R. Soc. Lond. Ser. Math. Phys. Sci.*, vol. 166, no. 924, pp. 16–43, Jan. 1997, doi: 10.1098/rspa.1938.0079.
21. A. Walter, J. G. Mannheim, and C. J. Caruana, Eds., *Imaging Modalities for Biological and Preclinical Research: A Compendium, Volume 1: Part I: Ex vivo biological imaging*. IOP Publishing, 2021. doi: 10.1088/978-0-7503-3059-6.
22. A. A and V. S, 'X-ray Diffraction (XRD) and Energy Dispersive Spectroscopy (EDS) Analysis of Silver Nanoparticles Synthesized from Erythrina Indica Flowers', *Nanosci. Technol. Open Access*, vol. 5, no. 1, Feb. 2018, Accessed: Feb. 05, 2025. [Online]. Available: https://symbiosisonlinepublishing.com/nanoscience-technology/
23. R. Dhir *et al.*, 'Plant-mediated synthesis of silver nanoparticles: unlocking their pharmacological potential–a comprehensive review', *Front. Bioeng. Biotechnol.*, vol. 11, p. 1324805, Jan. 2024, doi: 10.3389/fbioe.2023.1324805.
24. A. K. Mittal, J. Bhaumik, S. Kumar, and U. C. Banerjee, 'Biosynthesis of silver nanoparticles: Elucidation of prospective mechanism and therapeutic potential', *J. Colloid Interface Sci.*, vol. 415, pp. 39–47, Feb. 2014, doi: 10.1016/j.jcis.2013.10.018.

IRAQI Academic Scientific Journals
Samarra Journal of Pure and Applied Science
SJPAS
مجلة سامراء للعلوم البحتة والتطبيقية
www.sjpas.com
p ISSN: 2663-7405
e ISSN: 2789-6838

التخليق الأخضر لجسيمات الفضة النانوية باستخدام قشور الليمون لتصنيع مستشعر كهروكيميائي محسن للكشف عن السلفاميثوكسازول

مروان حامد لطيف[1]*، شذى يونس يحيى[2]
1- قسم الكيمياء التطبيقية، كلية العلوم التطبيقية، جامعة سامراء، العراق
2- قسم الكيمياء، كلية العلوم، جامعة تكريت، العراق

معلومات البحث:
تأريخ الاستلام: 27/ 04/2025
تاريخ التعديل : 24/05/2025
تأريخ القبــول: 06/06/2025
تاريخ الـنشر: 10/04/2026
الكلمات المفتاحية:
سلفاميثوكسازول، جسيمات الفضة النانوية ،التخليق الأخضر،المستشعر المطلي ،الكشف عن الأدوية

معلومات المؤلف
الايميل:
marwan.hamid@st.tu.edu.iq
الموبايل:07711717420

الخلاصة:
تم تطوير حساس كهروكيمياوي صديق للبيئة للكشف الانتقائي عن عقار السلفاميثوكسازول (SMX)، وهو أحد المضادات الحيوية من فئة السلفوناميدات، وذلك باستخدام جسيمات الفضة النانوية (AgNPs) المحضّرة بطريقة خضراء باستخدام مستخلص قشور الليمون. تم تشكيل معقّد مزدوج الأيون (SMX-AgNPs) بين AgNPs وSMX، ثم تم دمجه في قطب انتقائي للأيونات قائم على الغرافيت.وقد أُجريت عمليات التوصيف البنيوي والمورفولوجي للمواد النانوية المحضّرة باستخدام تقنيات مطيافية الأشعة فوق البنفسجية-المرئية (UV–Vis)، والمجهر الإلكتروني الماسح (SEM)، والتحليل الطيفي بالأشعة السينية المشتتة للطاقة (EDX)، والحيود بالأشعة السينية (XRD)، مما أكد تكوُّن جسيمات بلورية نانوية الحجم.أظهر القطب المصنع نطاق استجابة خطي واسعاً يتراوح من 1×10^{-1} إلى $\times10^{-7}$ مولاري، وزمن استجابة سريع، وقابلية تكرار عالية، مع الحفاظ على استقراره التشغيلي لمدة تصل إلى 65 يوماً. أبدى الحساس حساسية وانتقائية ممتازتين، مما مكّنه من التقدير الدقيق لـ SMX في المستحضرات الصيدلانية.
وتُبرز هذه النتائج الإمكانيات الواعدة لجسيمات الفضة النانوية المحضّرة بطريقة خضراء في تطوير تقنيات استشعار كهربائي-كيميائي منخفضة التكلفة ومستدامة لرصد الأدوية.